HHS Public Access

Author manuscript

J Neurosurg. Author manuscript; available in PMC 2016 November 02.

Published in final edited form as:

J Neurosurg. 2015 April ; 122(4): 791–797. doi:10.3171/2014.10.JNS14911.

High-resolution ^{18}F-fluorodeoxyglucose positron emission tomography and magnetic resonance imaging for pituitary adenoma detection in Cushing disease

Prashant Chittiboina, MD[1], **Blake K. Montgomery**[1], **Corina Millo, MD**[2], **Peter Herscovitch, MD**[2], and **Russell R. Lonser, MD**[1,3]

[1]Surgical Neurology Branch, National Institutes of Neurological Disorders and Stroke, Bethesda, Maryland [2]Positron Emission Tomography Department, Warren Grant Magnuson Clinical Center, National Institutes of Health, Bethesda, Maryland [3]Department of Neurological Surgery, The Ohio State University Wexner Medical Center, Columbus, Ohio

Abstract

OBJECT—High-resolution PET (hrPET) performed using a high-resolution research tomograph is reported as having a resolution of 2 mm and could be used to detect corticotroph adenomas through uptake of ^{18}F-fluorodeoxyglucose (^{18}F-FDG). To determine the sensitivity of this imaging modality, the authors compared ^{18}F-FDG hrPET and MRI detection of pituitary adenomas in Cushing disease (CD).

METHODS—Consecutive patients with CD who underwent preoperative ^{18}F-FDG hrPET and MRI (spin echo [SE] and spoiled gradient recalled [SPGR] sequences) were prospectively analyzed. Standardized uptake values (SUVs) were calculated from hrPET and were compared with MRI findings. Imaging findings were correlated to operative and histological findings.

RESULTS—Ten patients (7 females and 3 males) were included (mean age 30.8 ± 19.3 years; range 11–59 years). MRI revealed a pituitary adenoma in 4 patients (40% of patients) on SE and 7 patients (70%) on SPGR sequences. ^{18}F-FDG hrPET demonstrated increased ^{18}F-FDG uptake consistent with an adenoma in 4 patients (40%; adenoma size range 3–14 mm). Maximum SUV was significantly higher for ^{18}F-FDG hrPET–positive tumors (difference = 5.1, 95% CI 2.1–8.1; p = 0.004) than for ^{18}F-FDG hrPET–negative tumors. ^{18}F-FDG hrPET positivity was not associated

Correspondence: Prashant Chittiboina, Surgical Neurology Branch, National Institute of Neurological Diseases and Stroke, National Institutes of Health, 10 Center Dr., Rm. 3D20, Bethesda, MD 20892. prashant.chittiboina@nih.gov.

Clinical trial registration no.: NCT01459237 (clinicaltrials.gov)

Author Contributions

Conception and design: Chittiboina, Herscovitch, Lonser. Acquisition of data: Chittiboina, Montgomery, Millo. Analysis and interpretation of data: Chittiboina, Millo, Lonser. Drafting the article: Chittiboina. Critically revising the article: Chittiboina, Lonser. Reviewed submitted version of manuscript: Chittiboina, Millo, Lonser. Approved the final version of the manuscript on behalf of all authors: Chittiboina. Statistical analysis: Chittiboina. Study supervision: Herscovitch, Lonser.

Disclosure This study was funded by the intramural research program of the National Institute of Neurological Disorders and Stroke at the National Institutes of Health. This research was also made possible through the National Institutes of Health Medical Research Scholars Program, a public-private partnership supported jointly by the NIH, and generous contributions to the Foundation for the NIH from Pfizer Inc., The Doris Duke Charitable Foundation, The Alexandria Real Estate Equities, Inc., and Mr. and Mrs. Joel S. Marcus, and the Howard Hughes Medical Institute, as well as other private donors.

with tumor volume (p = 0.2) or dural invasion (p = 0.5). Midnight and morning ACTH levels were associated with ^{18}F-FDG hrPET positivity (p = 0.01 and 0.04, respectively) and correlated with the maximum SUV (R = 0.9; p = 0.001) and average SUV (R = 0.8; p = 0.01). All ^{18}F-FDG hrPET–positive adenomas had a less than a 180% ACTH increase and ^{18}F-FDG hrPET–negative adenomas had a greater than 180% ACTH increase after CRH stimulation (p = 0.03). Three adenomas were detected on SPGR MRI sequences that were not detected by ^{18}F-FDG hrPET imaging. Two adenomas not detected on SE (but no adenomas not detected on SPGR) were detected on ^{18}F-FDG hrPET.

CONCLUSIONS—While ^{18}F-FDG hrPET imaging can detect small functioning corticotroph adenomas and is more sensitive than SE MRI, SPGR MRI is more sensitive than ^{18}F-FDG hrPET and SE MRI in the detection of CD-associated pituitary adenomas. Response to CRH stimulation can predict ^{18}F-FDG hrPET–positive adenomas in CD.

Keywords

Cushing disease; pituitary adenoma; positron emission tomography; magnetic resonance imaging; pituitary surgery

Biochemical remission after transsphenoidal surgery in Cushing disease (CD) is influenced by the ability to visualize a pituitary adenoma on preoperative imaging. Currently, MRI is the gold standard for detecting pituitary microadenomas. Nevertheless, modern pituitary MRI sequences fail to detect a pituitary adenoma in approximately 40% of CD cases due to small tumor size and/or poor MRI contrast-to-noise ratio at the sella-sphenoid interface.[8,11] When adenomas are visible on preoperative imaging, remission rates approaching 90%–100% have been reported.[15,16] When adenomas are not detected on preoperative MRI, remission rates can decrease to 50%–60% in CD.[11,15,17]

Standard spin echo (SE) MRI sequences (pre- and postcontrast administration) have been and are currently used to image the pituitary gland for adenomas in CD. Using SE MRI, approximately 50% of adenomas in CD can be detected using preoperative postcontrast MRI studies.[14] Since 2003, the spoiled gradient recalled (SPGR) MRI sequence (pre- and postcontrast administration) has been used to best enhance detection of pituitary adenomas in CD.[2,10,11] While SPGR MRI has increased detection of pituitary adenomas in CD (a 10%–15% increase in sensitivity in CD adenoma detection), a large portion of pituitary adenomas in CD remain undetected on MRI before resection. [8,11,14]

To enhance detection of pituitary adenomas in patients with CD undergoing SE and/or SPGR MRI, investigators have used standard resolution (approximately 6-mm resolution) ^{18}F-fluorodeoxyglucose (^{18}F-FDG) PET imaging. Data from these MRI and PET studies revealed that ^{18}F-FDG PET is complementary to SE MRI in detecting pituitary adenomas not detected on preoperative MRI in 25% of CD cases.[1,4] Recently, technological advances have led to development of high-resolution PET (hrPET) using a high-resolution research tomograph scanner.[18] These scanners have a 2-mm resolution.[3] These advances suggest that hrPET scanners may be used to detect small biologically active adenomas in CD via ^{18}F-FDG uptake.[1,4]

Based on improvements in both MRI and PET as defined above, the combination of these 2 modalities may provide an opportunity to enhance detection of CD-associated pituitary adenomas. To assess the sensitivity of these imaging techniques for detection of CD-associated pituitary adenomas (alone and in a complementary fashion), we prospectively compared high-resolution MRI (SE and SPGR sequences) with ^{18}F-FDG hrPET for detection of corticotroph adenomas in CD. Furthermore, to determine if biological features of adenomas in CD could be used to predict ^{18}F-FDG uptake, we analyzed biological factors in patients with CD undergoing ^{18}F-FDG hrPET.

Methods

Patients

Patients with CD were enrolled in a clinical trial (registration no. NCT01459237) (clinicaltrials.gov) conducted at the National Institute of Neurological Diseases and Stroke (NINDS) (12-N-0007) to prospectively evaluate the use of ^{18}F-FDG hrPET for CD. All patients or guardians (in the case of minors) signed informed consent.

Diagnosis of CD

To distinguish between adrenocorticotropic hormone (ACTH)–dependent causes (either ectopic or pituitary) of hypercortisolism, patients underwent biochemical evaluation including high-dose dexamethasone testing, corticotropin-releasing hormone (CRH) stimulation testing, and MRI of the pituitary. Patients with high-dose dexamethasone suppression of cortisol, CRH-induced elevation of ACTH and cortisol, as well as MRI evidence of a pituitary adenoma were given a diagnosis of CD. Patients with negative findings on MRI or indefinite endocrinological evaluation underwent inferior petrosal sinus sampling (IPSS) to confirm or exclude a pituitary source of ACTH secretion.[13]

MRI of the Pituitary Gland

All patients underwent MRI of the pituitary gland before resection. MRI sequences included 3-mm SE sequences in coronal and sagittal orientation, as well as 1-mm 3D gradient echo (spoiled gradient or SPGR) sequence, as described previously.[14] Coronal T1-weighted SE scans were obtained using the following parameters: TR 400 msec, TE 9 msec, and 12-cm FOV. Contiguous 3-mm-thick slices were obtained. SPGR scans were performed using the following parameters: TR 9.6 msec, TE 2.3 msec, and 12-cm FOV. Contiguous 1-mm–thick coronal slices were obtained for SPGR sequences. MRI findings were assessed by a neuroradiologist before surgery for the presence of an adenoma. Adenoma volume was assessed by a formula calculating ellipsoid volume of brain tumors (volume = [maximal mediolateral dimension × maximal anteroposterior dimension × maximal vertical dimension]/2).[19]

^{18}F-FDG hrPET Protocol

PET imaging was performed using a high-resolution research tomography scanner (Siemens AG). Subjects were asked to fast (except water) for at least 6 hours prior to the imaging session. Commercially manufactured ^{18}F-FDG was injected intravenously over a period of approximately 1 minute. The ^{18}F-FDG dose was standardized at 10 mCi in patients who

were 18 years and older. For patients younger than 18 years, the dose was calculated at 0.08 mCi/kg. The subjects rested quietly in a dark room for approximately 30 minutes after ^{18}F-FDG administration. During the scan, a cap with small light reflectors was placed on the subject's head to monitor head position with a Polaris Vicra head tracking system (Northern Digital Inc.). Information about head movement was used in the image reconstruction process to reduce the blurring effect of head movement on the PET images. After the patient was positioned in the scanner, a transmission scan was obtained with a ^{137}Cesium rotating pin source to correct emission images for attenuation. Then a PET emission scan of the brain was obtained in 3D mode starting about 50 minutes after ^{18}F-FDG injection for up to 40 minutes. Standardized uptake values (SUVs) for ^{18}F-FDG were calculated after normalization of focal ^{18}F-FDG uptake for body weight and injected dose of ^{18}F-FDG.[12]

Surgical Procedure

All patients underwent a standard sublabial transsphenoidal approach for pituitary adenoma resection, as described previously.[9] Briefly, wide bony removal was performed at the sellar face and sellar floor until the cavernous sinuses were visualized. Once dura overlying the pituitary gland was opened, the exposed pituitary gland was inspected for the presence of tumor. The pituitary capsule was incised adjacent to the expected adenoma location. The pituitary pseudocapsule was developed to complete selective adenectomy. When cavernous sinus invasion was suspected, the involved medial wall of the cavernous sinus was removed.

Histopathology

Routine H&E staining was performed to evaluate the surgical specimens, as well as reticulin staining. ACTH immunostaining was performed to confirm the diagnosis of corticotroph adenoma.

Statistical Analysis

An unpaired t-test was used to detect a difference between the means. Fisher's exact test was used for analysis of contingency tables. Pearson correlation coefficients were calculated when generating correlation matrices for continuous variables. The McNemar test was used to compare sensitivities of diagnostic tests. Statistical significance was set at $p \leq 0.05$.

Results

Patients

Ten consecutive patients (7 females and 3 males) were included (mean age 30.8 ± 19.3 years [SD]; range 11–59 years) (Table 1). All patients were diagnosed with CD on the basis of clinical and biochemical criteria. While 1 patient presented with recurrent CD, 9 patients were diagnosed with new-onset CD (Table 1). All 10 patients underwent MRI of the pituitary gland and ^{18}F-FDG hrPET imaging before surgery.

Imaging Findings

MRI—A pituitary adenoma was visible in 4 patients using postcontrast SE MRI, and an adenoma was visible in 7 patients using SPGR MRI sequences. All pituitary adenomas that

were detected by SE MRI were also detected using SPGR MRI. Adenoma location on MRI corresponded with the surgical location of the adenoma in every case. There was no association between MRI adenoma detection and biochemical findings.

MRI Compared With ^{18}F-FDG hrPET Imaging—Three adenomas were detected on SPGR MRI but not on ^{18}F-FDG hrPET. ^{18}F-FDG hrPET did not detect any adenomas that SPGR MRI did not detect. All adenomas detected on SE MRI were detected by ^{18}F-FDG hrPET. Furthermore, ^{18}F-FDG hrPET detected 2 adenomas that were not detected by SE MRI (Table 1). These 2 adenomas were 3 and 5 mm in diameter (Fig. 1). Adenoma location on ^{18}F-FDG hrPET–positive imaging corresponded with the surgical location of the adenoma.

^{18}F-FDG hrPET Imaging

Increased SUVs corresponding to an adenoma were detected in 4 patients. The maximum SUV (SUV_{Max}) in ^{18}F-FDG hrPET–positive adenoma ranged from 6.0 to 12.8 (mean 9.5 ± 1.6) (Table 2). The average SUV (SUV_{Avg}) in the sella ranged from 2.3 to 4.0 (mean 3.1 ± 0.4) in ^{18}F-FDG hrPET–positive cases. SUV_{Max} in ^{18}F-FDG hrPET–negative cases ranged from 3.7 to 5.0 (mean 4.4 ± 0.2). SUV_{Avg} for sella ranged from 2.0 to 2.8 (mean 2.5 ± 0.1) in ^{18}F-FDG hrPET–negative cases. While SUV_{Max} was significantly higher for ^{18}F-FDG hrPET–positive adenomas ($p = 0.004$) compared with ^{18}F-FDG hrPET–negative adenomas, SUV_{Avg} was not ($p = 0.08$).

Factors Associated With ^{18}F-FDG Uptake

^{18}F-FDG hrPET positivity was not associated with age ($p = 0.1$), sex ($p = 0.2$), presence of dural invasion ($p = 0.5$), or adenoma volume ($p = 0.2$). ^{18}F-FDG hrPET positivity was associated with midnight and morning ACTH levels ($p = 0.01$ and $p = 0.04$, respectively). Both midnight and morning ACTH values correlated with SUV_{Max} ($R = 0.9$, $p = 0.001$) and SUV_{Avg} ($R = 0.8$, $p = 0.01$) (Fig. 2). There was no association between the IPSS central-to-peripheral ratio and ^{18}F-FDG hrPET positivity ($p = 0.79$) or maximum central ACTH values ($p = 0.2$). Basal IPSS ACTH values were higher in ^{18}F-FDG hrPET–positive tumors (mean 534 ± 439 pg/ml) than in ^{18}F-FDG hrPET–negative tumors (mean 70.63 ± 25.95 pg/ml), but the difference was not statistically significant ($p = 0.2$).

CRH stimulation demonstrated that change in ACTH level after stimulation (mean of 15 and 30 minutes) was significantly less in ^{18}F-FDG hrPET–positive tumors (mean change 112.2 ± 31.8%) than in ^{18}F-FDG hrPET–negative tumors (mean change 237.9 ± 32.8%; $p = 0.03$). All ^{18}F-FDG hrPET–positive tumors were associated with an increase in ACTH after stimulation less than 180%, and all ^{18}F-FDG hrPET–negative tumors had an increase in ACTH after stimulation greater than 180% (Fig. 3). No association was found with cortisol response to CRH stimulation ($p = 0.8$) with ^{18}F-FDG hrPET–positive tumors.

Surgical and Clinical Findings

Surgical Findings—A pituitary adenoma was found in all cases at surgery. Adenoma location on MRI corresponded with the surgical location of the tumor. Similarly, adenomas seen on ^{18}F-FDG hrPET corresponded with surgical findings. Maximum adenoma diameter

ranged from 3 to 14 mm (mean 6.2 ± 3.5 mm). Adenoma volume ranged from 12.0 to 336.0 mm^3 (mean 106.9 ± 128.4 mm^3). Invasion of the adjacent dura was identified in 3 cases (anterior sella dura in 1 case and medial cavernous sinus wall in 2 cases).

Clinical Results—All patients achieved biochemical remission after surgery. Briefly, biochemical remission was defined by postoperative morning serum cortisol and 24-hour urinary free cortisol. Patients achieved either a reduction of serum cortisol below 5 μg/dl and urinary free cortisol below the reference range (hypocortisolemia) or within the reference range (eucortisolemia).[11] Histology confirmed an ACTH-positive adenoma in all cases.

Discussion

MRI in CD

Adoption of SPGR MRI sequences led to an increased sensitivity (80%) compared with SE MRI sequences (49%).[14] The SPGR MRI technique utilizes faster acquisition times leading to minimal movement and pulsation artifacts. Although a lower signal-to-noise ratio is reported for SPGR sequences than for SE sequences, a higher contrast-to-noise ratio is achievable. Moreover, SPGR MRI allows for 1-mm–thick sections, which can potentially permit detection of smaller adenomas.[14] Subsequently, SPGR MRI is superior for detecting smaller tumors that have a contrast difference relative to the normal pituitary gland. For these reasons, we have found that SPGR MRI provides optimal detection of pituitary adenomas in CD patients.[2,11,14]

Biological Rationale for ^{18}F-FDG PET in CD

Large series of whole-body ^{18}F-FDG PET imaging have examined the features that underlie incidental ^{18}F-FDG uptake in the sella. They found that ^{18}F-FDG uptake in the pituitary gland is found in less than 0.1% of cases.[5,7] More than 95% of these patients had an underlying pituitary adenoma detected on MRI as a source of increased ^{18}F-FDG uptake.[7] These findings demonstrated that ^{18}F-FDG PET imaging of the pituitary gland/sella has high specificity for detection of pituitary adenomas[5] and could potentially be used for detection of pituitary adenomas in this region. Specifically, these prior data suggested that ^{18}F-FDG PET imaging could be exploited to detect biologically (high metabolic) active CD-associated adenomas that suppress the metabolic activity of the surrounding pituitary gland.

Based on the pituitary findings from whole-body ^{18}F-FDG PET imaging and the biological features of CD-associated adenomas, groups have used standard resolution ^{18}F-FDG PET imaging in CD patients for adenoma detection. These studies found that in 25% of cases, ^{18}F-FDG PET imaging played a complementary role to SE MRI, detecting ACTH-secreting adenomas that were not visible on SE MRI.[1,4] Furthermore, no false-positive cases were reported with the use of ^{18}F-FDG PET imaging in CD in these series.[1,4] Nevertheless, some lesions not detected using ^{18}F-FDG PET imaging were visualized on SE MRI, but no biological explanation for these results was established that would improve understanding of the application of the ^{18}F-FDG PET imaging modality.

Here, we analyzed the effectiveness of ^{18}F-FDG hrPET imaging (2-mm resolution) and biological factors associated with ^{18}F-FDG hrPET imaging positivity in patients with CD.

Current Study

Sensitivity of Imaging Modalities—Consistent with previous data,[14] the findings in the current study showed an improvement in adenoma detection sensitivity from 40% to 70% with SPGR over standard SE MRI sequences. The sensitivity of ^{18}F-FDG hrPET was 40% for the detection of CD adenomas in the current series, which was less than the sensitivity (70%) of SPGR MRI techniques for detection of pituitary adenomas in this series of patients with CD. Similarly, previous studies reported an advantage of ^{18}F-FDG PET over SE MRI sequences, as we found in the current series.[1,4] Nevertheless, we found no advantage of ^{18}F-FDG hrPET over high-resolution SPGR MRI. These data underscore the effectiveness of SPGR MRI for detecting ACTH-secreting adenomas in CD.

Regardless of the imaging modality, when an adenoma was identified it corresponded with the location (side of gland) and size of the tumor. These findings indicate that methods to improve the sensitivity of either MRI or PET will not only assist in diagnosis but will have direct surgical implications. Specifically, any of these modalities, including ^{18}F-FDG hrPET, can guide surgical exploration (and perhaps partial hypophysectomy) to the correct location within the pituitary gland and enhance effectiveness of resection. This is particularly important for very small (2 mm in diameter or less) imaging-invisible CD-associated adenomas that have not formed a pseudocapsule[6] and may be difficult to distinguish from normal pituitary gland.

Biological Implications—Previous studies in CD have not detected an association with biochemical markers for ACTH-secreting adenomas and ^{18}F-FDG uptake using standard-resolution PET imaging.[1,4] Similar to De Souza colleagues[4] (who used standard-resolution PET imaging), we did not find an association between IPSS findings and ^{18}F-FDG uptake. Likewise, we did not find an association between IPSS findings and ^{18}F-FDG positivity. While Alzahrani and colleagues[1] did not find an association between ^{18}F-FDG uptake using standard PET imaging, we found an association between ^{18}F-FDG hrPET positivity and quantitative ^{18}F-FDG uptake with midnight and morning ACTH levels. The differences between our findings and those of Alzahrani and colleagues[1] could be due to resolution of the PET imaging used and/or the timing of ACTH sampling (timing is not reported in the study by Alzahrani and colleagues).

These correlations (ACTH level association with ^{18}F-FDG uptake) reveal intrinsic variability among CD-associated adenomas. Specifically, adenomas that comparatively and constitutively oversecrete ACTH, as demonstrated by higher midnight ACTH, may respond less to diurnal hypothalamic commands and have a higher metabolic signature leading to increased ^{18}F-FDG uptake. These findings are underscored by the reduced sensitivity of ^{18}F-FDG hrPET–positive adenomas to CRH stimulation. ^{18}F-FDG hrPET–positive adenomas had a significantly attenuated response to CRH stimulation compared with ^{18}F-FDG hrPET–negative adenomas (Fig. 3). Adenomas that have increased constitutive overexpression of ACTH and increased glucose uptake may have an attenuated response to CRH stimulation (i.e., less responsive to CRH stimulation).

Clinical Implications

The findings of the current study demonstrate that the biochemical phenotype of CD-associated adenomas plays the largest role in ^{18}F-FDG PET positivity. Specifically, biological aspects have a larger role than adenoma size or dural invasion in determining ^{18}F-FDG uptake. These findings are supported by preoperative biochemical findings and the detection of very small adenomas (3 mm in diameter) by ^{18}F-FDG hrPET imaging but lack of detection of larger and more CRH stimulation responsive adenomas. Consequently, it is possible that biological features can be exploited to apply ^{18}F-FDG hrPET imaging in cases with comparatively blunted responses to CRH stimulation (less than 180% increase of ACTH; Fig. 3) and high midnight ACTH levels that do not have evidence of an adenoma on SPGR MRI. In such circumstances, it is possible that ^{18}F-FDG hrPET imaging could play a noninvasive diagnostic role (versus IPSS).

Conclusions

^{18}F-FDG hrPET can detect functioning corticotroph adenomas as small as 3 mm in size. While ^{18}F-FDG hrPET allowed for detection of small adenomas in CD, it offers no advantages over SPGR MRI sequences. High midnight ACTH level and an attenuated response to CRH stimulation can predict ^{18}F-FDG hrPET–positive adenomas in CD.

Abbreviations

ACTH	adrenocorticotropic hormone
CD	Cushing disease
CRH	corticotropin-releasing hormone
hrPET	high-resolution PET
IPSS	inferior petrosal sinus sampling
SE	spin echo
SPGR	spoiled gradient recalled
SUV	standardized uptake value
SUV_{Avg}	average SUV
SUV_{Max}	maximum SUV

References

1. Alzahrani AS, Farhat R, Al-Arifi A, Al-Kahtani N, Kanaan I, Abouzied M. The diagnostic value of fused positron emission tomography/computed tomography in the localization of adrenocorticotropin-secreting pituitary adenoma in Cushing's disease. Pituitary. 2009; 12:309–314. [PubMed: 19387839]
2. Chowdhury IN, Sinaii N, Oldfield EH, Patronas N, Nieman LK. A change in pituitary magnetic resonance imaging protocol detects ACTH-secreting tumours in patients with previously negative results. Clin Endocrinol (Oxf). 2010; 72:502–506. [PubMed: 19500112]

3. de Jong HW, van Velden FH, Kloet RW, Buijs FL, Boellaard R, Lammertsma AA. Performance evaluation of the ECAT HRRT: an LSO-LYSO double layer high resolution, high sensitivity scanner. Phys Med Biol. 2007; 52:1505–1526. [PubMed: 17301468]
4. De Souza B, Brunetti A, Fulham MJ, Brooks RA, DeMichele D, Cook P, et al. Pituitary microadenomas: a PET study. Radiology. 1990; 177:39–44. [PubMed: 2399336]
5. Hyun SH, Choi JY, Lee KH, Choe YS, Kim BT. Incidental focal 18F-FDG uptake in the pituitary gland: clinical significance and differential diagnostic criteria. J Nucl Med. 2011; 52:547–550. [PubMed: 21421711]
6. Jagannathan J, Smith R, DeVroom HL, Vortmeyer AO, Stratakis CA, Nieman LK, et al. Outcome of using the histological pseudocapsule as a surgical capsule in Cushing disease. J Neurosurg. 2009; 111:531–539. [PubMed: 19267526]
7. Jeong SY, Lee SW, Lee HJ, Kang S, Seo JH, Chun KA, et al. Incidental pituitary uptake on whole-body 18F-FDG PET/CT: a multicentre study. Eur J Nucl Med Mol Imaging. 2010; 37:2334–2343. [PubMed: 20661556]
8. Kasaliwal R, Sankhe SS, Lila AR, Budyal SR, Jagtap VS, Sarathi V, et al. Volume interpolated 3D-spoiled gradient echo sequence is better than dynamic contrast spin echo sequence for MRI detection of corticotropin secreting pituitary microadenomas. Clin Endocrinol (Oxf). 2013; 78:825–830. [PubMed: 23061773]
9. Kerr PB, Oldfield EH. Sublabial-endonasal approach to the sella turcica. J Neurosurg. 2008; 109:153–155. [PubMed: 18590448]
10. Kucharczyk W, Bishop JE, Plewes DB, Keller MA, George S. Detection of pituitary microadenomas: comparison of dynamic keyhole fast spin-echo, unenhanced, and conventional contrast-enhanced MR imaging. AJR Am J Roentgenol. 1994; 163:671–679. [PubMed: 8079866]
11. Lonser RR, Wind JJ, Nieman LK, Weil RJ, DeVroom HL, Oldfield EH. Outcome of surgical treatment of 200 children with Cushing's disease. J Clin Endocrinol Metab. 2013; 98:892–901. [PubMed: 23372173]
12. Lucignani G, Paganelli G, Bombardieri E. The use of standardized uptake values for assessing FDG uptake with PET in oncology: a clinical perspective. Nucl Med Commun. 2004; 25:651–656. [PubMed: 15208491]
13. Nieman LK, Biller BM, Findling JW, Newell-Price J, Savage MO, Stewart PM, et al. The diagnosis of Cushing's syndrome: an Endocrine Society Clinical Practice Guideline. J Clin Endocrinol Metab. 2008; 93:1526–1540. [PubMed: 18334580]
14. Patronas N, Bulakbasi N, Stratakis CA, Lafferty A, Oldfield EH, Doppman J, et al. Spoiled gradient recalled acquisition in the steady state technique is superior to conventional postcontrast spin echo technique for magnetic resonance imaging detection of adrenocorticotropin-secreting pituitary tumors. J Clin Endocrinol Metab. 2003; 88:1565–1569. [PubMed: 12679440]
15. Prevedello DM, Pouratian N, Sherman J, Jane JA Jr, Vance ML, Lopes MB, et al. Management of Cushing's disease: outcome in patients with microadenoma detected on pituitary magnetic resonance imaging. J Neurosurg. 2008; 109:751–759. [PubMed: 18826366]
16. Rees DA, Hanna FW, Davies JS, Mills RG, Vafidis J, Scanlon MF. Long-term follow-up results of transsphenoidal surgery for Cushing's disease in a single centre using strict criteria for remission. Clin Endocrinol (Oxf). 2002; 56:541–551. [PubMed: 11966748]
17. Semple PL, Vance ML, Findling J, Laws ER Jr. Transsphenoidal surgery for Cushing's disease: outcome in patients with a normal magnetic resonance imaging scan. Neurosurgery. 2000; 46:553–559. [PubMed: 10719850]
18. van Velden FH, Kloet RW, van Berckel BN, Buijs FL, Luurtsema G, Lammertsma AA, et al. HRRT versus HR+ human brain PET studies: an interscanner test-retest study. J Nucl Med. 2009; 50:693–702. [PubMed: 19372482]
19. Yu YL, Lee MS, Juan CJ, Hueng DY. Calculating the tumor volume of acoustic neuromas: comparison of ABC/2 formula with planimetry method. Clin Neurol Neurosurg. 2013; 115:1371–1374. [PubMed: 23375462]

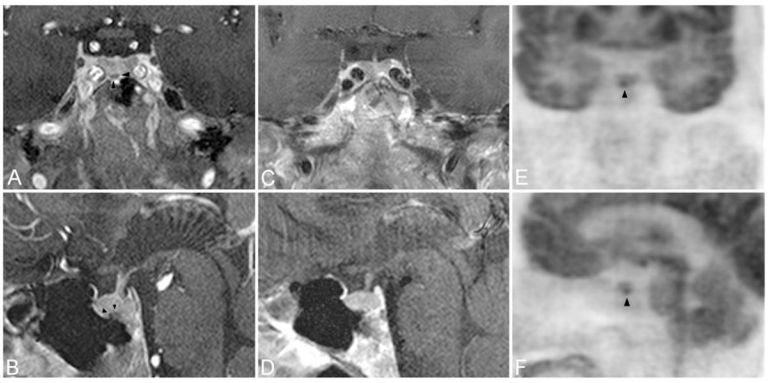

Fig. 1.

Images obtained in a patient in whom a hypoenhancing adenoma *(arrowheads)* was detected on SPGR sequences **(A and B)**, but not on SE sequences **(C and D)**. Corresponding ^{18}F-FDG hrPET images **(E and F)** revealed a focus of increased ^{18}F-FDG uptake *(arrowhead)*.

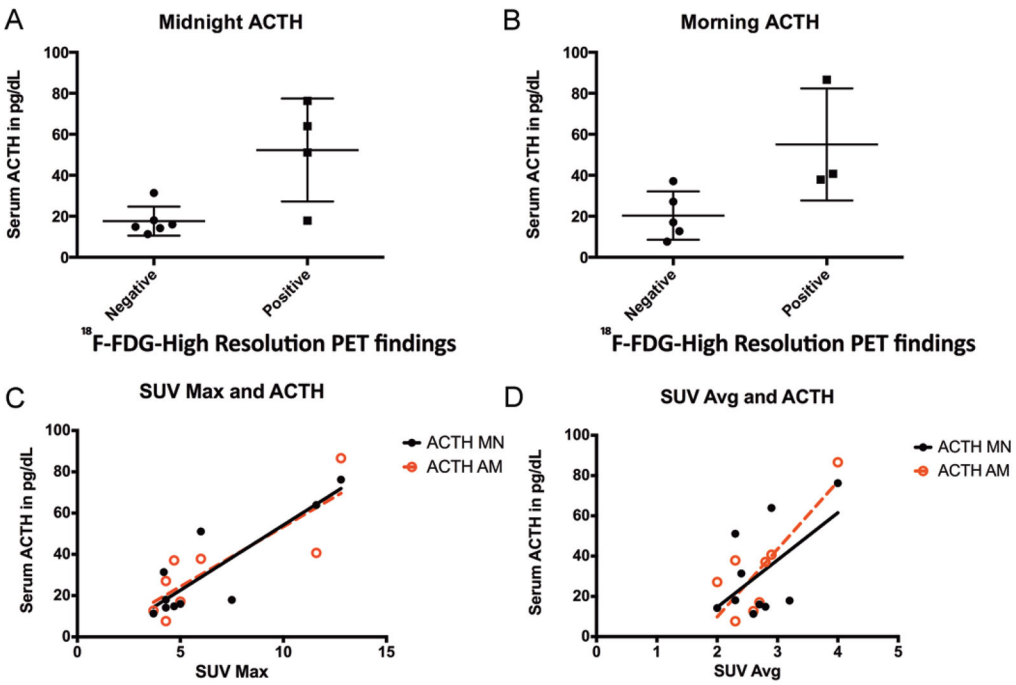

Fig. 2.

A and B: ^{18}F-FDG hrPET findings were associated with biochemical data. Tumors detected on ^{18}F-FDG hrPET had higher midnight (A) and morning (B) serum ACTH levels. **C and D:** Correlation between serum ACTH (*black,* midnight [MN]; *red,* morning [AM]) with both maximum SUV (SUV Max; C) and average SUV (SUV Avg; D) for the sella.

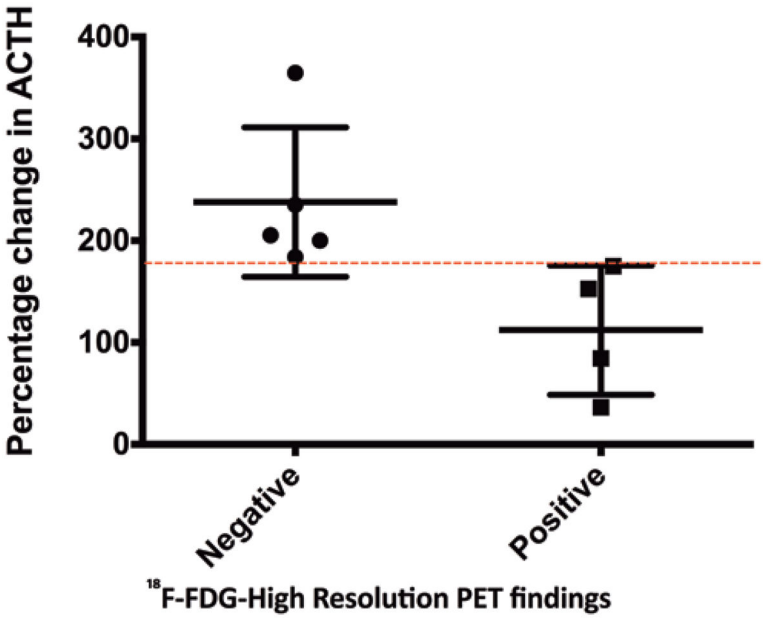

Fig. 3.

^{18}F-FDG hrPET–positive tumors had an attenuated response to CRH stimulation. All ^{18}F-FDG hrPET–positive tumors had an attenuated response, specifically, less than 180% change in ACTH level during CRH stimulation test. The *red line* demonstrates cutoff at 180% change that separates the ^{18}F-FDG hrPET–positive tumors from negative tumors.

TABLE 1

Summary statistics for the patients in this study*

Case No.	Age (yrs), Sex	CD Diagnosis	Max Dia (mm)	Vol (mm^3)	Invasion	MRI SPGR	MRI SE	hrPET
1	15, F	New	5	30	No	No	No	No
2	37, F	New	14	336	Yes	Yes	Yes	Yes
3	13, M	New	3	13.5	No	No	No	No
4	15, M	New	4	16	No	Yes	Yes	No
5	59, F	New	10	320	Yes	Yes	Yes	Yes
6	37, F	Recurrent	6	108	Yes	Yes	No	No
7	58, F	New	3	13.5	No	Yes	No	Yes
8	15, F	New	5	40	No	Yes	No	Yes
9	48, F	New	4	12	No	Yes	Yes	No
10	11, M	New	10	180	No	No	No	No

*Max Dia indicates maximum diameter of adenoma at surgery; Vol, volume of adenoma calculated at surgery; Invasion, presence of invasion noted at surgery; MRI SPGR, presence of hypoenhancing tumor noted on SPGR sequence preoperatively; MRI SE, presence of hypoenhancing tumor noted on SE sequence preoperatively; hrPET, presence of adenoma detected by increased FDG uptake preoperatively.

TABLE 2

Summary statistics for differences in tumors that were positive or negative on ^{18}F-FDG hrPET

	^{18}F-FDG hrPET*		
Variable	**Positive**	**Negative**	**p Value**
Age in yrs	42.25 ± 10.40	23.17 ± 6.306	0.10
Sex (female/male)	4/0	3/3	0.20
Dural invasion (present/absent)	2/2	5/1	0.50
Vol in mm^3	177.4 ± 87.19	59.92 ± 28.29	0.17
SUV_{Max}	9.475 ± 1.621	4.367 ± 0.1820	0.004†
SUV_{Avg}	3.100 ± 0.3536	2.467 ± 0.1202	0.08
ACTH MN in pg/ml	52.30 ± 12.56	17.63 ± 2.89	0.01†
ACTH AM in pg/ml	55.05 ± 15.80	20.32 ± 5.27	0.04†
Cortisol MN in mg/dl	20.90 ± 4.16	15.09 ± 2.82	0.26
Cortisol AM in mg/dl	23.04 ± 5.69	19.35 ± 4.43	0.62
Diurnal variation in ACTH in pg/ml	−11.01 ± 7.40	−0.70 ± 7.65	0.38
Diurnal variation in cortisol	2.13 ± 3.15	1.03 ± 4.47	0.86
Basal IPSS ACTH in pg/ml	534.1 ± 439.0	70.6 ± 25.9	0.16
Maximum IPSS ACTH in pg/ml	11826 ± 10811	1036 ± 427.7	0.18
Maximum IPSS gradient in pg/ml	46.72 ± 16.33	60.66 ± 33.18	0.80
ACTH % rise w/CRH stimulation	112.2 ± 31.76	237.9 ± 32.79	0.03†
Cortisol % rise w/CRH stimulation	362.8 ± 153.9	321.5 ± 78.91	0.81
ACTH-to-cortisol ratio	3.134 ± 0.68	2.693 ± 0.81	0.69

AM = morning; MN = midnight.

*All values are the means ± SD except for sex and dural invasion variables. These values are the number of patients.

†Statistically significant ($p < 0.05$).